ARTICLES
PUBLISHED ONLINE: 26 MAY 2013 | DOI: 10.1038/NPHOTON.2013.109
nature photonics

Phase-conjugated twin waves for communication beyond the Kerr nonlinearity limit

Xiang Liu*, A. R. Chraplyvy, P. J. Winzer, R. W. Tkach and S. Chandrasekhar

Kerr nonlinearity imposes a limit on the achievable transmission performance and capacity of optical fibre communication links. We show that the nonlinear distortions of a pair of phase-conjugated twin waves are essentially anticorrelated, so cancellation of signal-to-signal nonlinear interactions can be achieved by coherently superimposing the twin waves at the end of the transmission line. We demonstrate that by applying this approach to fibre communication, nonlinear distortions can be reduced by >8.5 dB. In dispersive nonlinear transmission, the nonlinearity cancellation additionally requires a dispersion-symmetry condition that can be satisfied by appropriately predispersing the signals. By using these techniques we succeed in transmitting a 400 Gb s^{-1} superchannel over 12,800 km of fibre. We further show a connection between the nonlinearity cancellation and a nonlinear noise squeezing effect. The concept of using phase-conjugated twin waves to suppress nonlinear interactions may prove beneficial in other physical systems governed by the nonlinear Schrödinger equation.

Optical fibre communication has enabled the exponential growth in communication capacity of the information era. The theoretical capacity upper bound of a linear communication link is set by the Shannon limit[1]. As optical fibre transmission capacity continues to increase[2,3], so does the optical signal power required to ensure sufficient signal-to-noise ratio (SNR), which results in signal distortions due to fibre Kerr nonlinearity[4–6]. Fibre Kerr nonlinearity thus imposes an upper bound on the maximum effective SNR of a link, and limits the achievable transmission performance. There have been extensive efforts attempting to break the Kerr nonlinear limit through nonlinearity compensation[7–12], which has limitations such as the inability to mitigate interchannel nonlinear impairments when the *E*-field evolution of other wavelength-division multiplexed channels is unknown to the compensator, and demonstrates impractically high complexity when numerous computation steps are needed to undo the nonlinear interactions, as in the case of dispersive transmission. Mid-link optical phase conjugation (ML-PC) is a well-known technique for compensating for chromatic dispersion[13], nonlinearity[14] and the combined effect of chromatic dispersion and nonlinearity[15–18] by performing phase conjugation on the *E*-field of each optical signal near the middle of a transmission link. However, ML-PC requires the transmission link to be modified by inserting a phase conjugator inside the link, and requires near mirror-imaged power evolutions about the phase conjugator, which significantly reduces the flexibility of optically routed networks.

Here, we propose a method to realize the cancellation of nonlinear signal-to-signal interactions by transmitting a pair of mutually phase-conjugated twin waves (PCTWs) together through a nonlinear medium, and coherently superimposing them at the receiver site. When modulating a pair of PCTWs on two orthogonal polarizations of a same optical carrier via quadrature phase-shift keying (QPSK), we demonstrate nonlinear distortion reductions of >8.5 dB when both dispersion and linear noise (for example, amplified spontaneous noise, ASE) are negligibly small. For dispersive nonlinear transmission, the nonlinearity cancellation also requires a dispersion-symmetry condition that can be satisfied by appropriately predispersing the signals, for example by means of electronic dispersion precompensation (pre-EDC). Using the PCTW concept, we transmit a 400 Gb s^{-1} superchannel consisting of eight pairs of PCTWs modulated by 32-Gbaud QPSK over a record distance of 12,800 km in a TrueWave reduced slope (TWRS) fibre link consisting of 80 km of terrestrial-type spans that are amplified only by erbium-doped fibre amplifiers (EDFAs). We further show that the nonlinearity cancellation effect can be interpreted as a beneficial nonlinear noise squeezing (NLNS) effect under a unitary transformation.

Basic principle

The schematic of a PCTW-based transmission link, where the twin waves are co-propagating on two orthogonal polarizations of the same optical carrier, is shown in Fig. 1a. For comparison, a transmission link with ML-PC is shown in Fig. 1b. To visualize how the PCTW-based nonlinearity cancellation works, in Fig. 1c we show the simulated evolutions of the *E*-field distortions of the twin waves E_x and E_y during nonlinear propagation. A detailed description of the simulation method is presented in the Methods. Evidently, the nonlinear distortion δE_x on E_x is essentially anticorrelated with δE_y^*, the nonlinear distortion of its twin after phase conjugation (so as to be coherently superimposed with E_x), E_y^*. As such, upon optical or digital electronic coherent superposition[19] of E_x and a polarization-rotated copy of E_y^* at the receiver, the *E*-field of the original signal is expected to be restored without nonlinear distortions. This mechanism is fundamentally different from that of ML-PC, where the nonlinear distortion that has occurred in the first half of the transmission link is time-reversed in the second half of the link (compare the trajectories of field distortions in Fig. 1d).

To theoretically explain the PCTW-enabled nonlinearity cancellation, we start with the coupled nonlinear Schrödinger equations[20] that govern the nonlinear optical propagation of a polarization-division multiplexed (PDM) vector wave $\mathbf{E} = (E_x, E_y)^T$ in an optical fibre, which, under the common assumption that the nonlinear interaction length is much greater than the length scale of random polarization rotations, can be reduced to the Manakov

Bell Labs, Alcatel-Lucent, 791 Holmdel-Keyport Road, Holmdel, New Jersey 07733, USA. *e-mail: xiang.liu@alcatel-lucent.com

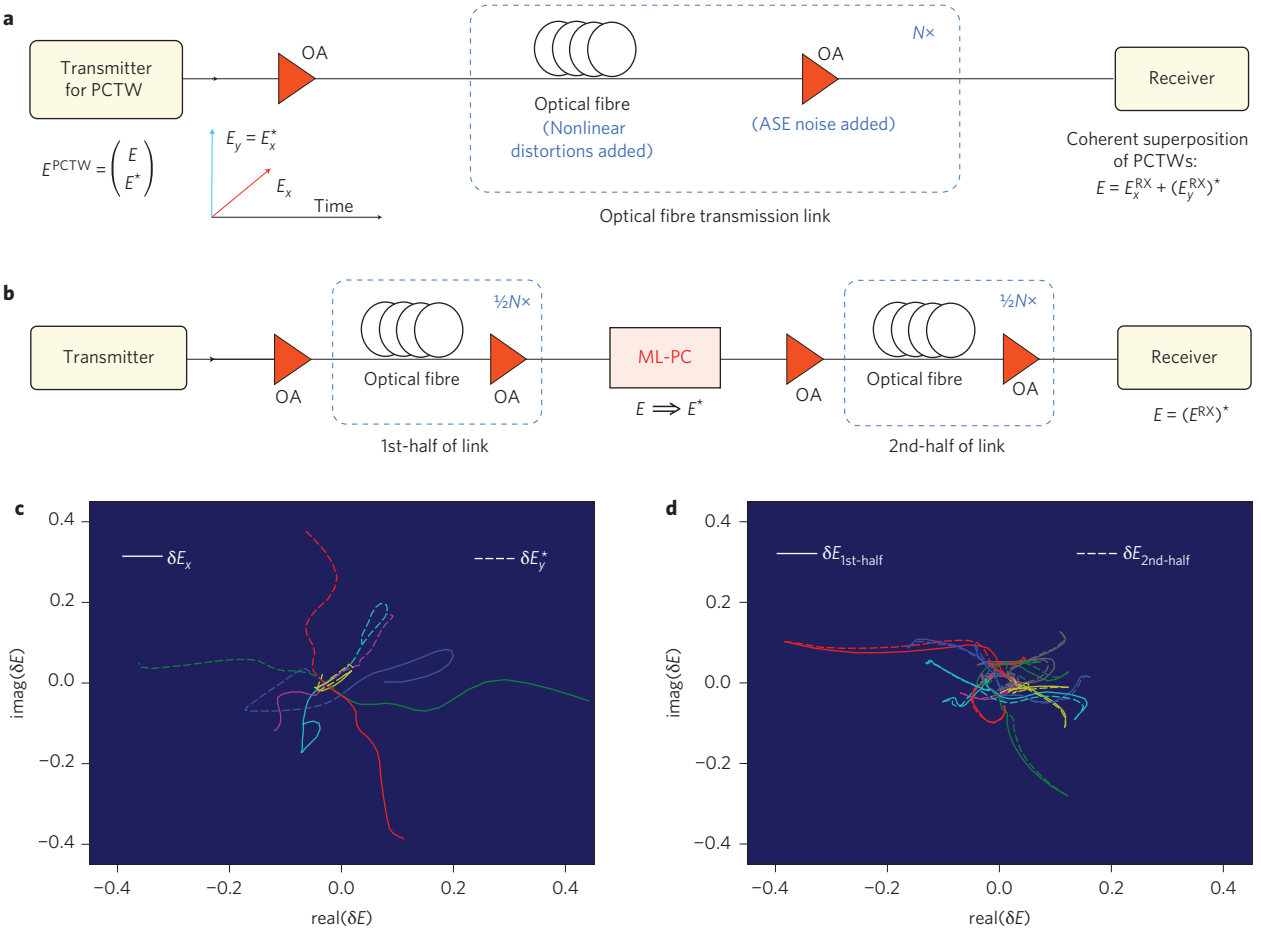

Figure 1 | Illustration of nonlinearity cancellation based on PCTWs and comparison with ML-PC. a, Schematic of a transmission link with a pair of PCTWs (E and E^*) co-propagating on two orthogonal polarizations of the same optical carrier. The received twin waves (E_x^{RX} and E_y^{RX}) are coherently superimposed to restore the original signal field. OA, optical amplifier. **b**, Schematic of a transmission link incorporating ML-PC. **c**, Simulated evolutions of the distortions of the PCTWs (δE_x and δE_y^*) in a fibre link for a representative set of consecutive symbols. We use the same colour for distortions occurring on the same symbol to show that δE_x is essentially anticorrelated with its corresponding δE_y^*. It is this symmetry between δE_x and δE_y^* about the origin that enables the nonlinearity cancellation. **d**, Simulated signal distortion evolutions in the ML-PC case with the same fibre link as in **c**.

equation as[21]

$$\left[\frac{\partial}{\partial z}+\frac{\alpha(z)-g(z)}{2}+i\frac{\beta_2(z)}{2}\frac{\partial^2}{\partial t^2}\right]E_{x,y}(z,t)=i\tfrac{8}{9}\gamma\left(|E_x(z,t)|^2+|E_y(z,t)|^2\right)E_{x,y}(z,t) \quad (1)$$

where i is the imaginary unit, and z, α, g, β_2 and γ, respectively, are the propagation distance, the loss coefficient, the gain coefficient, the group-velocity dispersion (or second-order dispersion) coefficient, and the fibre nonlinear Kerr coefficient along a transmission link. Extending the previously reported perturbation approach[22–25], we can express the nonlinear distortions after transmission in the frequency domain (to first order) as

$$\begin{aligned}\delta E_{x,y}(L,\omega)=i\tfrac{8}{9}\gamma P_0 L_{\text{eff}}\int_{-\infty}^{+\infty}\mathrm{d}\omega_1\int_{-\infty}^{+\infty}\mathrm{d}\omega_2\,\eta(\omega_1\omega_2)\\ \times\left[E_{x,y}(\omega+\omega_1)E_{x,y}(\omega+\omega_2)E^*_{x,y}(\omega+\omega_1+\omega_2)\right.\\ \left.+E_{y,x}(\omega+\omega_1)E_{x,y}(\omega+\omega_2)E^*_{y,x}(\omega+\omega_1+\omega_2)\right]\end{aligned} \quad (2)$$

where $E_{x,y}(\omega)=\int_{-\infty}^{\infty}E_{x,y}(0,t)e^{-i\omega t}\mathrm{d}t/\sqrt{2\pi}$, and $G(z)=\int_0^z[g(z')-\alpha(z')]\,\mathrm{d}z'$, $L_{\text{eff}}=\int_0^z e^{G(z)}\mathrm{d}z$ and $C(z)=\int_0^z\beta_2(z')\,\mathrm{d}z'$ are the logarithmic signal power evolution, the effective length and the cumulative dispersion along the link, respectively, and $\eta(\omega_1\omega_2)$ is the dimensionless nonlinear transfer function[23,25], defined as

$$\eta(\omega_1\omega_2)=\int_0^L\exp[G(z)-i\omega_1\omega_2C(z)]\,\mathrm{d}z/L_{\text{eff}}$$

In the above derivations, we assume that the E-fields of the PCTWs after transmission are normalized in power and post-compensated to be free of residual dispersion. When a symmetric dispersion map is applied such that $C(z)=-C(L-z)$, $G(z)=G(L-z)$, $\eta(\omega_1\omega_2)$ becomes real-valued[24,25]. Note that a symmetric dispersion map in a dynamic optical networking environment can be readily obtained by performing pre-EDC at the transmitter, through techniques such as software-defined digital electronic dispersion compensation. For PCTW-based transmission, we have the relations

$$E_y(0,t)=E_x(0,t)^*,\quad E_y(\omega)=E_x^*(-\omega)$$

Closely inspecting equation (2) and using $\eta(\omega_1\omega_2)=\eta(\omega_1\omega_2)^*$, we then have (for PCTW-based transmission with a symmetric dispersion map)

$$\delta E_y(L,\omega)=-[\delta E_x(L,-\omega)]^*,\ \delta E_y(L,t)=-[\delta E_x(L,t)]^* \quad (3)$$

indicating that the nonlinear distortions experienced by the PCTWs

are anticorrelated. It is this anticorrelation that leads to the first-order cancellation of nonlinear distortions and restoration of the original signal field, $E(0,t)$, upon coherent superposition the received PCTWs:

$$E_x(L,t) + E_y(L,t)^* = 2E(0,t)$$

A remarkable feature is that the nonlinear signal distortions that can be cancelled include those resulting from the interaction between Kerr nonlinearity and dispersion. In addition, as abundantly exploited in many fields of physics and engineering, the coherent superposition halves[19] the variance of linear noise resulting from ASE, further improving the overall signal quality.

Single-channel experiment

To experimentally verify the PCTW-based nonlinear cancellation, we first conducted an experiment with non-dispersive transmission (Fig. 2a). The PCTWs were modulated with QPSK at 10 Gb s^{-1} onto two orthogonal polarization components of an optical carrier at 1,550 nm. The phase conjugation was performed in the time domain by means of transmitter-side digital signal processing. The predispersion compensation of the PCTWs was conducted in the digital domain before driving the modulator. A 20 km standard single-mode fibre (SSMF) with a nonlinear Kerr coefficient of 1.27 W^{-1} km^{-1} and a dispersion coefficient of ~17 ps nm^{-1} km^{-1} was used as the transmission medium, resulting in negligible dispersion-induced pulse broadening. A key parameter that characterizes the nonlinear effect experienced by the PCTWs is the mean phase shift (Φ_{NL}), defined as $\Phi_{NL} = \gamma P_{in} L_{eff}$, where P_{in} is the signal launch power into each fibre span, which can be varied by adjusting the gain of the preceding optical amplifier. After transmission, the E-fields of the PCTWs were recovered by a coherent receiver, followed by coherent superposition of the twin waves. A more detailed description of the experimental set-up is presented in the Methods. At the medium power level corresponding to $\Phi_{NL} \approx 0.6$ rad, the overall signal variance (σ^2) is reduced by over tenfold upon coherent superposition of the recovered PCTWs (Fig. 2b), much more than the reduction measured at low power levels (approximately twofold), confirming the expected nonlinear cancellation through PCTW. The variance here is calculated by averaging the variances measured for the angular and radial distortions. Representative recovered PCTW constellations before and after the coherent superposition are also shown for nearly linear transmission (Fig. 2c) and for nonlinear transmission (Fig. 2d). The reduction in the nonlinear distortion-induced signal variance (measured after removing the linear noise variance resulting from digitization noise and ASE noise) is even more pronounced, achieving over 13 dB (20-fold) reduction at $\Phi_{NL} \approx 0.6$ rad. The nonlinear cancellation becomes less effective as Φ_{NL} increases, indicating that full cancellation may be hindered by higher-order perturbation terms.

We also conducted an experiment with highly dispersive transmission (Fig. 3a). The transmission link was replaced with a 3,200 km SSMF link, which was constructed by using a recirculating loop consisting of four optically amplified 80 km SSMF spans. The dispersion coefficient D, length L and accumulated dispersion $D \times L$ of the link were 17 ps nm^{-1} km^{-1}, 3,200 km and 54,400 ps nm^{-1}, respectively. As presented above, the dispersion map needs to be symmetric to attain the full benefit of the PCTW-based nonlinearity cancellation. A symmetric dispersion map can be realized by appropriately performing pre- and post-dispersion compensation, either optically or electronically, at the transmitter and receiver sites, without modifying the transmission link itself, which is in sharp contrast to the ML-PC approach. In this experiment, we

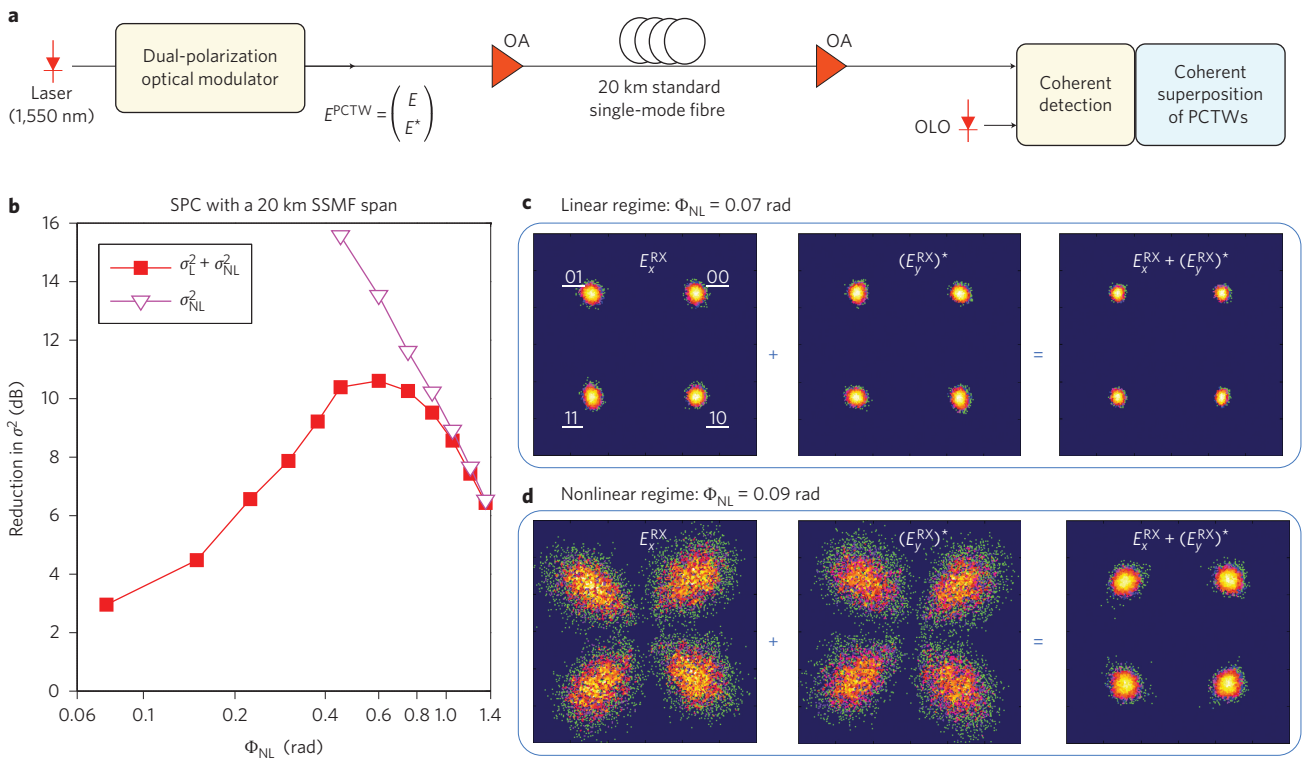

Figure 2 | Experimental observation of nonlinearity cancellation in non-dispersive transmission. a, Schematic of experimental set-up. The optical modulator is a polarization-multiplexed inphase/quadrature (I/Q) modulator with four electric inputs to address sine and cosine components of the E-field in both x- and y-polarizations of an optical carrier at 1,550 nm. OLO, optical local oscillator. **b**, Measured reduction of signal variance from both nonlinear distortions (σ_{NL}^2) and linear noise (σ_L^2). **c**, Recovered PCTW optical field distributions (sampled for each modulation symbol) before and after coherent superposition in a nearly linear transmission scenario, indicating a signal variance reduction of ~3 dB. **d**, Recovered PCTW constellations before and after coherent superposition in a nonlinear transmission scenario, indicating a dramatic variance reduction of ~10 dB.

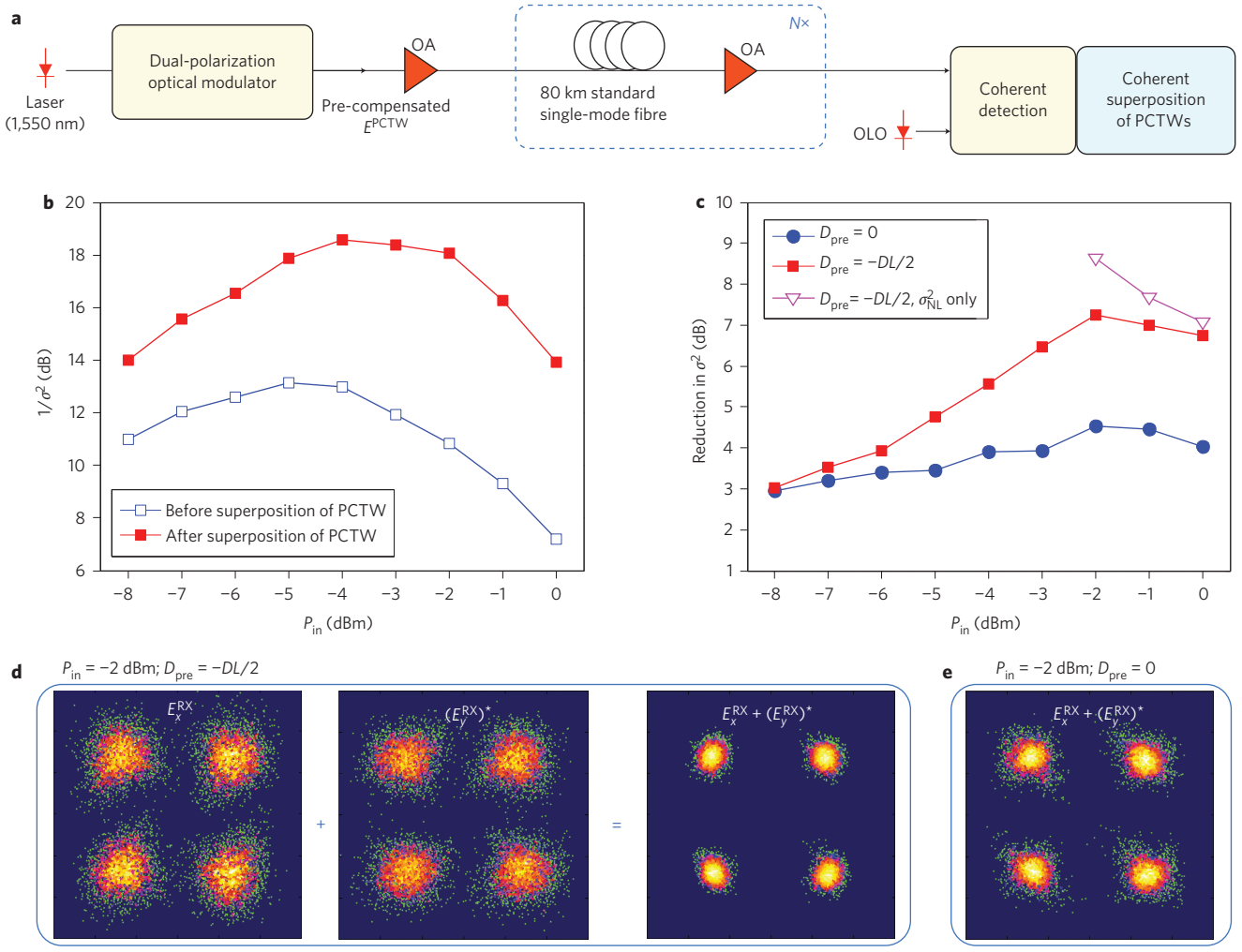

Figure 3 | Experimental observation of nonlinearity cancellation in highly dispersive transmission. a, Schematic of experimental set-up. To make the dispersion map symmetric, pre- and post-dispersion compensations of the PCTWs are applied at the transmitter and the receiver, respectively. **b**, Measured $1/\sigma^2$ as a function of P_{in}. **c**, Measured signal variance reduction versus P_{in}. **d**, Recovered PCTW constellations before and after coherent superposition with the symmetric dispersion map at $P_{in} = -2$ dBm, indicating a signal variance reduction of >7 dB. **e**, Recovered constellation after coherent superposition of PCTW with the asymmetric dispersion map at $P_{in} = -2$ dBm, confirming the benefit of having a symmetric dispersion map.

precompensated half of the fibre link dispersion ($D_{pre} = -D \times L/2$) using transmitter-side digital signal processing (DSP), and post-compensated the residual dispersion at the receiver. A key quality measure of a received signal is the inverse of the variance of signal distortions ($1/\sigma^2$) when the signal power is normalized to unity. Figure 3b shows the quality factor ($1/\sigma^2$) as a function of signal launch power into each fibre span (P_{in}). At $P_{in} = -8$ dBm, the transmission is nearly linear, and the variance reduction after coherent superposition of the PCTWs is ~3 dB (Fig. 3c), as expected. At $P_{in} = -2$ dBm, the transmission is nonlinear (with $\Phi_{NL} \approx 0.6$ rad), and the overall variance reduction after coherent superposition becomes ~7.3 dB, which corresponds to a reduction of nonlinear signal variance of ~8.6 dB when the impact of the linear noise is excluded. The nonlinear variance reduction is slightly smaller than that obtained in the first experiment. We attribute this to increased polarization-mode dispersion (PMD) and polarization-dependent loss (PDL) in long-haul transmission, which make the twin waves less balanced, and reduces the effectiveness of the nonlinear cancellation. Another performance measure is bit error ratio (BER). With P_{in} between −7 dBm and −1 dBm, the BER measured after superposition of PCTW is zero (given the limited statistics of the captured 10^5-symbol sequences), so we are unable to use BER to quantify the performance improvement. However, non-zero BER values are measured at $P_{in} = -8$ dBm and 0 dBm, and the improvements in the Q-factors derived from the BER values are in agreement with the improvements seen using $1/\sigma^2$. We will show more BER results in section 'Multichannel WDM experiment' where more stringent nonlinear transmission conditions are used. To show the benefit of making the dispersion map symmetric, we compare the above results with those obtained without pre-dispersion compensation ($D_{pre} = 0$) in Fig. 3c. Indeed, the signal variance reduction achieved using the symmetric dispersion map (Fig. 3d) is much higher than that achieved using an asymmetric dispersion map (Fig. 3e), consistent with the theory.

Connection between PCTW and NLNS

In the special case where the PCTWs are synchronously modulated onto two polarization states of an optical carrier, we can link the PCTWs to polarization-division-multiplexed binary phase-shift keying (PDM-BPSK) through a unitary transformation

$$\begin{pmatrix} B_1(0,t) \\ B_2(0,t) \end{pmatrix} = \frac{1}{\sqrt{2}} \begin{pmatrix} 1 & 1 \\ -i & i \end{pmatrix} \begin{pmatrix} E(0,t) \\ E^*(0,t) \end{pmatrix} = \sqrt{2} \begin{pmatrix} \text{real}(E(0,t)) \\ \text{imag}(E(0,t)) \end{pmatrix}$$

where $B_1(0,t)$ and $B_2(0,t)$ are two independent BPSK signals that are real-valued (without loss of generality) and orthogonally polarized,

and the unitary transmission matrix U is $(1\ 1; -i\ i)/\sqrt{2}$. After nonlinear transmission over distance L, we have, for the symmetric dispersion map case,

$$\begin{pmatrix} B_1(L,t) \\ B_2(L,t) \end{pmatrix} \approx \frac{1}{\sqrt{2}} \begin{pmatrix} 1 & 1 \\ -i & i \end{pmatrix} \begin{pmatrix} E(0,t) + \delta E_x(L,t) \\ E^*(0,t) - [\delta E_x(L,t)]^* \end{pmatrix}$$
$$= \begin{pmatrix} B_1(0,t) \\ B_2(0,t) \end{pmatrix} + i\sqrt{2} \begin{pmatrix} \mathrm{imag}(\delta E_x(L,t)) \\ -\mathrm{real}(\delta E_x(L,t)) \end{pmatrix}$$

In the above derivation, we used equation (3), $\delta E_y(L,t) = -[\delta E_x(L,t)]^*$; that is, the nonlinear distortions of the PCTWs are anticorrelated. Evidently, the nonlinear distortions on the PDM-BPSK signal are purely imaginary, or 'squeezed' such that the nonlinear distortions are 'parallel' to the decision boundary of BPSK, and hence do not penalize signal demodulation (under the first-order perturbation assumption). As such, the nonlinearity cancellation effect in the case of PCTW transmission is physically linked to a beneficial NLNS effect under a unitary transformation. Note that the term 'noise' is used loosely here, as the nonlinear distortions in dispersion-unmanaged coherent transmission can be approximately regarded as additive Gaussian noise[26,27]. The term 'squeezing' is used just to illustrate the effect, although it shows an intriguing similarity to the squeezing of quantum states[28], which has been found to provide striking benefits in some applications.

To experimentally observe the NLNS effect, we transmitted a pair of PCTWs with an increased modulation rate of 15 Gbaud and an increased transmission distance of 6,400 km (80×80 km SSMF spans)[29]. The signal launch power was 0 dBm. To realize a nearly symmetric dispersion map, we used pre-EDC with $D_{\mathrm{pre}} = -54{,}400$ ps nm^{-1}. Figure 4 shows the recovered PCTW constellations after digital coherent superposition (DCS) without and with pre-EDC, in comparison with their corresponding PDM-BPSK constellations obtained by applying the unitary transformation on the received PCTWs. As expected, the nonlinearity cancellation effect in the symmetric dispersion map case (cf. the leftmost subplots in Fig. 4a,b) is transformed to the beneficial NLNS effect (compare the two rightmost subplots Fig. 4a). The measured BER was 4×10^{-3} (with 1×10^6 bits processed) without pre-EDC ($D_{\mathrm{pre}} = 0$), and no errors were found for $D_{\mathrm{pre}} = -54{,}400$ ps nm^{-1}, clearly confirming the benefits of the NLNS.

Two-channel experiment

We conducted a two-channel wavelength-division multiplexing (WDM) experiment to study the tolerance of the PCTW to interchannel nonlinear impairments (Fig. 5a). A second wavelength channel was multiplexed with the original channel with a spacing of 0.4 nm to co-propagate through the 3,200 km SSMF link. Both channels carried decorrelated 10 Gb s^{-1} PCTW signals. We fixed the launch power of the original signal to −3 dBm, and varied the power of the interferer from −3 dBm to 3 dBm. This can be derived from the results shown in Fig. 5b, where, as the power of the interferer increases from −3 dBm to 3 dBm, the interchannel nonlinearity-induced noise variance increases by 0.095 before superposition and by 0.025 after superposition, indicating a reduction of 5.8 dB in the interchannel nonlinearity-induced noise variance. Figure 5c shows the received PCTW constellations before and after coherent superposition. The effectiveness of the PCTW in mitigating interchannel nonlinear impairments can be attributed to the fact that the twin waves see a very similar nonlinear environment formed by the interfering WDM channels. The improvement of signal tolerance to interchannel nonlinearity without knowing or manipulating other channels is a unique feature of the PCTW-based

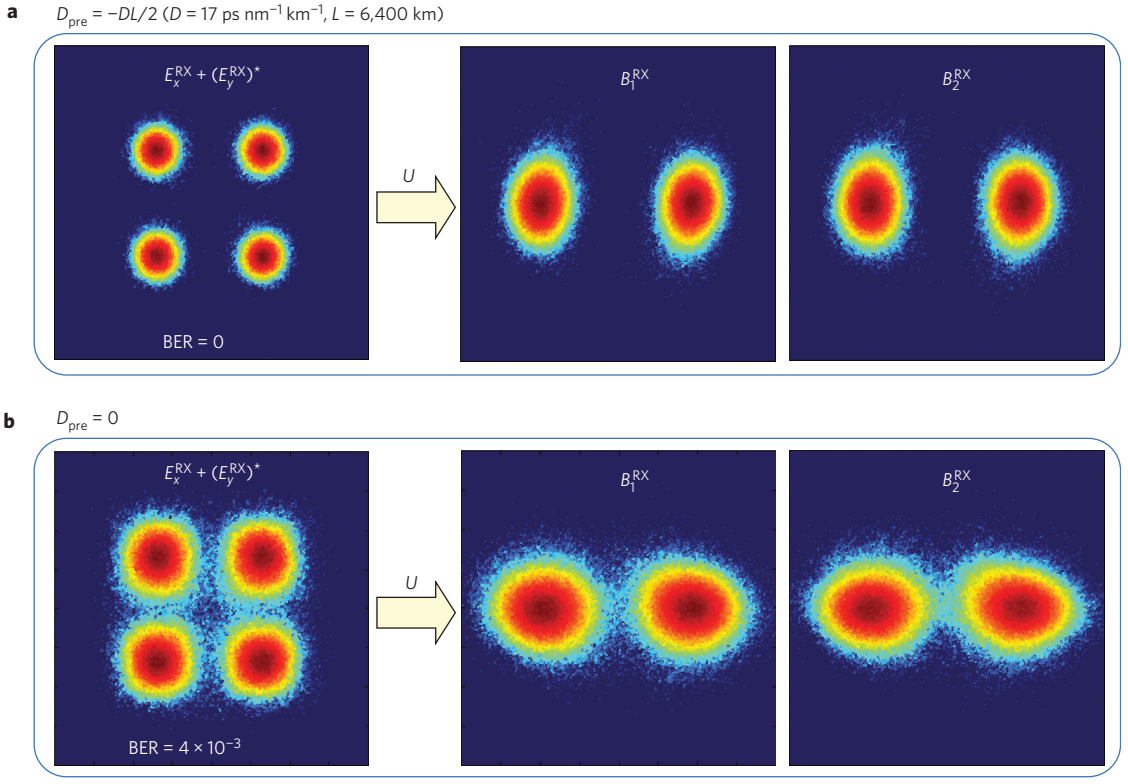

Figure 4 | Experimentally observed connection between nonlinearity cancellation and nonlinear noise squeezing. a, Recovered constellations of the PCTWs after coherent superposition and the transformed PDM-BPSK constellations after 6,400 km SSMF transmission with pre-EDC ($D_{\mathrm{pre}} = -54{,}400$ ps nm^{-1}). **b**, Recovered constellations after transmission over the same link without applying pre-EDC.

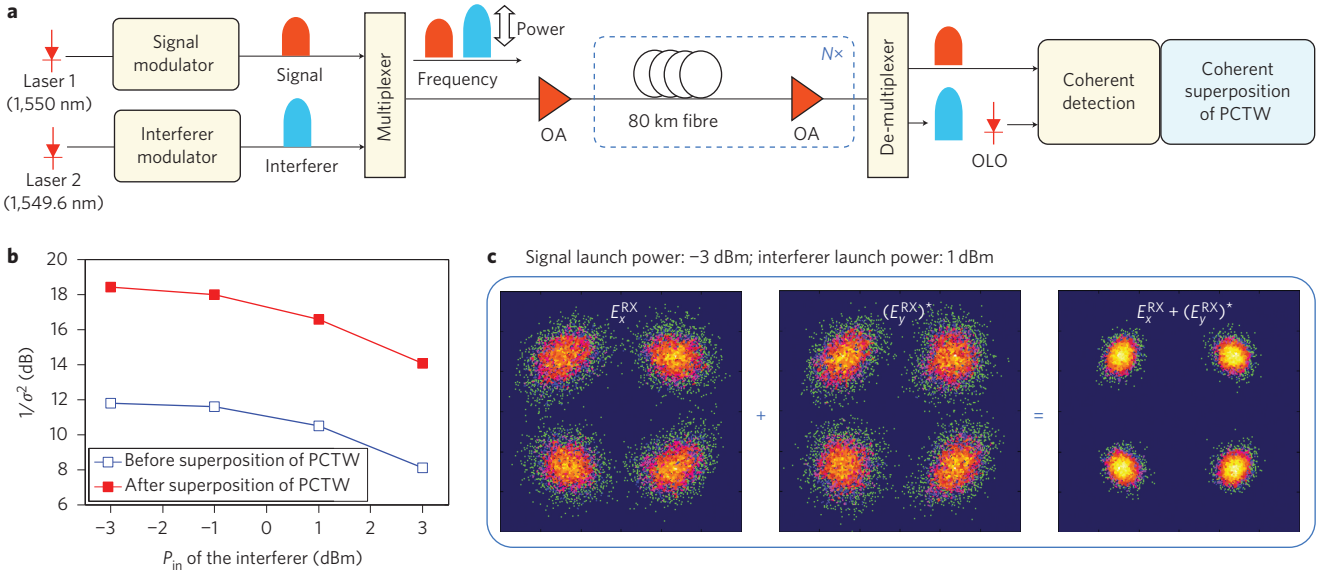

Figure 5 | Experimental verification of improved nonlinear tolerance to interchannel impairments. a, Schematic of experimental set-up. A second WDM channel is added to co-propagate with the original signal. **b**, Measured $1/\sigma^2$ as a function of the neighbouring channel power. **c**, Recovered PCTW constellations before and after coherent superposition, with the neighbouring channel having 4 dB higher power, showing the effectiveness of PCTW in mitigating interchannel nonlinear impairments.

transmission and is unattainable by conventional nonlinear compensation techniques.

It is of value to estimate the benefit of PCTW in addressing the Kerr nonlinearity limit. In dispersion-unmanaged transmission, the signal Q-factor improvement directly translates into reach improvement[26,27]. Based on the experimental results shown in Fig. 3 and additional measurements with conventional PDM-QPSK (Supplementary Fig. S1), the improvement in the optimum signal Q-factor obtained by the coherent superposition of PCTW is ~5.7 dB. For a communication link where the transmission distance requirement can be just met by the PCTW, the conventional PDM-QPSK signal (with doubled data rate for the same occupied optical bandwidth) would need to be regenerated three times along the link, thus requiring four optical transceivers for each signal. Further assuming that the 50% link capacity loss of the PCTW is compensated by using two parallel links[30] to achieve the same capacity–distance product, the total number of optical transceivers needed in the PCTW case would be 50% fewer than that in the PDM-QPSK case. As the cost of the optical transceivers is usually the dominating portion of the overall link cost, the use of PCTW would provide substantial cost saving in such ultralong-haul transmission applications. Moreover, for transmission links where signal regeneration inside the link is not allowed, for example, transoceanic optical links, the performance improvement brought by PCTW may be deemed valuable.

Multichannel WDM experiment

We next proceeded to quantify the benefit of PCTW under stringent nonlinear transmission conditions by performing high-spectral-efficiency superchannel transmission with eight pairs of closely spaced QPSK-modulated PCTWs over TWRS fibre spans[29]. The fibre dispersion and nonlinear Kerr coefficients were 4.66 ps nm^{-1} km^{-1} and 1.79 W^{-1} km^{-1}, respectively. Figure 6a presents a schematic of the experimental set-up. The modulation speed of the PCTW was further increased to 32 Gbaud using 64 GSamples/s (GSa s^{-1}) digital-to-analog converters (DACs). The channel spacing was 37.5 GHz, which is compatible with the emerging flexible-grid WDM architecture (ITU-T G.694.1). To achieve such close channel spacing, a root-raised-cosine filter with a roll-off factor of 0.1 was used to confine the optical spectra of the signals. The raw data rate of the superchannel was 512 Gb s^{-1}. After allocating 23.46% overhead for forward-error correction (FEC)[31], including an inner soft-decision[32] (SD) and an outer hard-decision (HD) code, and 2% overhead for training symbols and pilots, the net data rate became 406.6 Gb s^{-1}. Compared to the lower-rate experiment described earlier, this second experiment exhibits not only enhanced intrachannel nonlinear effects, but also substantial interchannel nonlinear effects. Figure 6b shows the Q^2-factor of the centre channel, derived from the measured BER, versus the signal launch power after 8,000 km (100 × 80 km) TWRS fibre transmission. At $P_{in} = -2$ dBm, the signal Q^2-factor obtained after DCS of the PCTW (DCS-PCTW) is 7.9 dB, which is ~5.2 dB higher than that of conventional PDM-QPSK. The improvement in terms of the optimal Q^2-factor is ~4 dB. Note that for the PCTW transmission, pre-EDC with $D_{pre} = -18{,}400$ ps nm^{-1} was applied to make the dispersion map nearly symmetric. We also found that a change of the D_{pre} value by ±2% did not cause a noticeable change in PCTW performance.

With the improved nonlinear transmission performance, we then transmitted the 406.6 Gb s^{-1} superchannel over a record distance of 12,800 km (160 × 80 km). Figure 6c shows the transmission performance of all eight channels comprising the superchannel performance after the 12,800 km TWRS transmission with $D_{pre} = -29{,}440$ ps nm^{-1}. The transmission penalty in terms of optical SNR was estimated to be ~3 dB. All eight channels inside the superchannel had a raw BER below 2.5×10^{-2}, and error-free performance was obtained (with 1×10^6 bits processed per measurement) even before applying the outer HD-FEC[33], the threshold of which was $\sim 4 \times 10^{-3}$. The PCTW generated in the experiment can also be interpreted as a PDM-BPSK signal using the unitary transformation described earlier, and the performance improvement can be seen as the result of the beneficial NLNS effect[29]. This demonstration further confirms the enhanced nonlinear transmission performance brought by PCTW under stringent transmission conditions with substantial interchannel nonlinear effects, PMD and PDL.

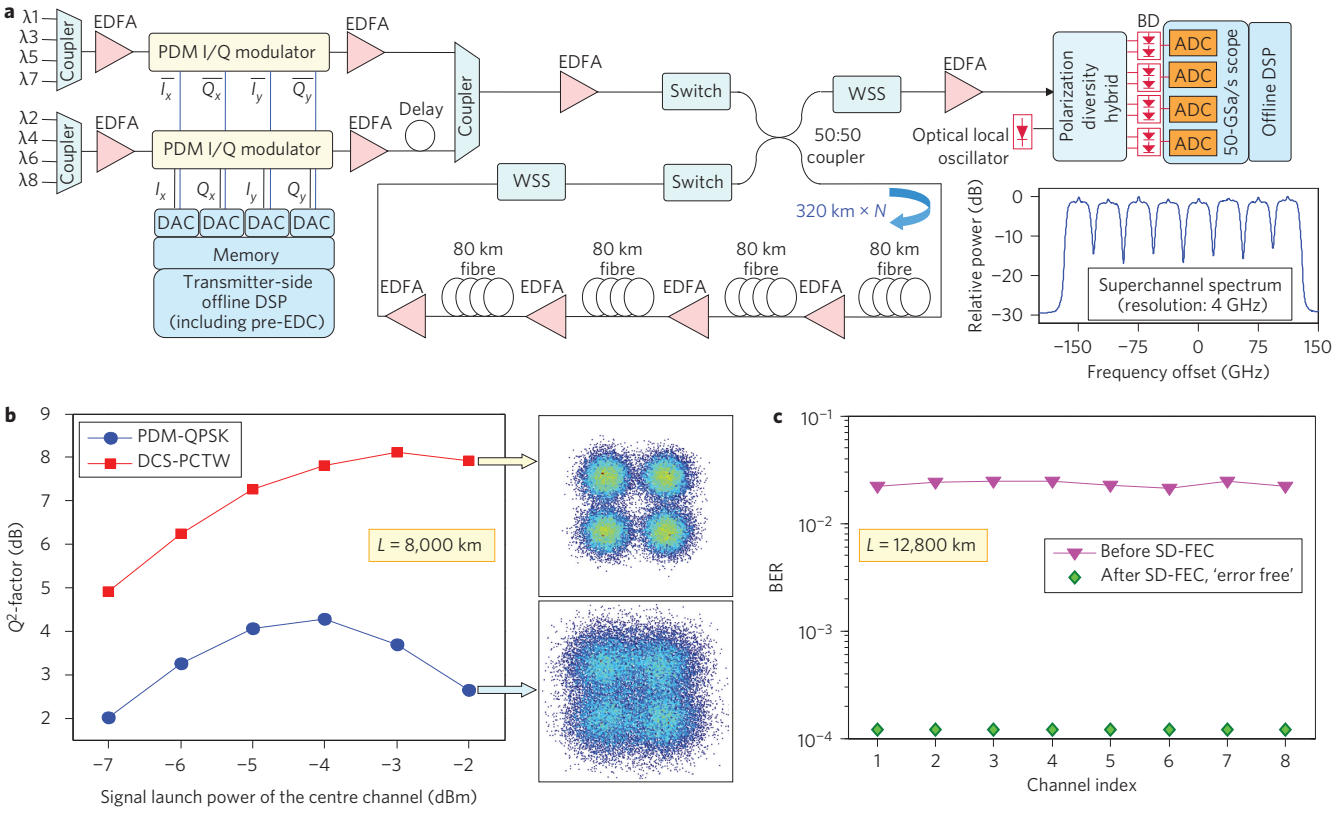

Figure 6 | Superchannel transmission with improved nonlinear transmission performance provided by PCTW. a, Schematic of experimental set-up. Inset: superchannel spectrum measured at the transmitter with 4 GHz resolution. **b**, Measured signal Q^2-factor (derived from the BER) as a function of the centre channel signal launch power after 8,000 km TWRS fibre transmission. Inset: recovered constellations. **c**, Measured BER after 12,800 km TWRS transmission at $P_{in} = -3$ dBm with optimized pre-EDC. BD, balanced detector; WSS, wavelength-selective switch PDM I/Q modulator, polarization-division-multiplexed inphase/quadrature modulator.

Discussion

To further mitigate interchannel nonlinear impairments, one could either increase the spectral bandwidth of the PCTWs to weaken the impact of the interchannel interactions or collaboratively modulate the WDM channels such that they collectively form a pair of PCTWs; for example, one polarization component of the channels is phase-conjugated as a whole with respect to the other polarization component. The latter case is well suited for the emerging superchannel transmission architecture[34,35] in which a group of closely packed signals are transmitted together over the same link. To efficiently perform dispersion precompensation for wide-bandwidth PCTW, a multiband compensation approach[36] may be used.

Rather than occupying two orthogonal polarizations of a same optical carrier, the PCTWs can propagate on different spatial paths. Multicore fibres have recently been used for space division multiplexing[37–39]. Transmitting PCTWs through different spatial paths may also be exploited to enhance the security of communication, for example by allowing for reliable communication only when both twins are simultaneously detected and coherently superimposed. The concept of PCTW can further be extended such that each of the twin waves is a vector wave (or a PDM signal) that contains two independently modulated polarization components.

We note that the beneficial NLNS effect is also applicable to other one-dimensional (1D) modulation formats such as m-ary pulse-amplitude modulation (m-PAM) for achieving higher spectral efficiency. Note also that this squeezing effect is not applicable to complex-valued modulation formats such as QPSK, so dispersion precompensation was not found to benefit the performance of PDM-QPSK[40], although the perturbation analysis may be applied for digital compensation of fibre nonlinear effects in an efficient manner. It can be shown that a pair of PCTWs using m^2-ary quadrature-amplitude modulation (m^2-QAM) can be transformed to PDM-m-PAM. Knowing the connection between the PCTWs and the NLNS effect, we can simply transmit a pair of PCTWs by using two independent (or uncorrelated) 1D signals that are polarization multiplexed. On the other hand, the built-in redundancy (or correlation) in PCTW offers the flexibility of transmitting the twin waves separately, for example on two different spatial paths.

Moreover, the PCTW may be naturally compatible with the emerging class of low-noise phase-sensitive amplifiers, based on the interaction between a signal and its phase-conjugated copy[41,42] in parametric optical amplification, to provide modulation-format-independent amplification and to improve communication immunity to both nonlinear distortions and linear noise.

The general concept has some resemblance to the recently demonstrated use of twin matter waves to achieve an interferometric sensitivity that is ~1.6 dB beyond the classical shot noise limit[43], and may also open new possibilities in other physical systems that are governed by the nonlinear Schrödinger equation in general, such as the recently discovered Higgs-like boson whose field dynamics can be modelled by the nonlinear Schrödinger equation[44] and whose predominant decay modes include the generation of a pair of photons[45,46].

Methods

Simulation. Figure 1c shows the simulated *E*-field distortion evolutions of the PCTW, E_x and E_y (where $E_y = E_x^*$), during nonlinear propagation to visualize how the PCTW-based nonlinearity cancellation works. The simulation was based on the standard symmetric split-step Fourier method[20] for solving the nonlinear Schrödinger equation, equation (1), in which dispersion is handled in the frequency

domain while nonlinearity is processed in the time domain. The simulation step size was one-tenth of a span and after each step the polarizations were randomly rotated and delayed in phase. The *E*-fields of the PCTWs were modulated with QPSK using pseudo random bit sequences (PRBS) of length $2^{11}-1$ at 10 Gb s^{-1}, and their time-domain waveforms were over-sampled by a factor of 2. The simulated transmission link consisted of up to forty 80 km SSMF spans with a dispersion coefficient D of 17 ps nm^{-1} km^{-1}. For a given link length L, the accumulated link dispersion ($D \times L$) was fully compensated by using pre- and post-dispersion compensation, each of which compensated for an equal amount of dispersion, $-D \times L/2$, so as to realize the symmetric dispersion mapping needed for optimizing the performance of PCTW-based transmission. At the receiver, the *E*-fields of the PCTWs were recovered via channel equalization, using the estimated channel response obtained from some known training symbols. To obtain the evolution of the *E*-fields of the PCTW at different link lengths, the above wave propagation and equalization process was repeated from a one-span link to a forty-span link with a nonlinear phase shift of 0.025 rad per span. To focus on the signal distortions due to fibre nonlinearity, no optical noise was added in the simulated transmission link. The *E*-field distortions of the PCTWs were then obtained by comparing the recovered *E*-fields with the original *E*-fields. The evolutions of the *E*-field distortions, $\delta E_x(L,t)$ and $\delta E_y^*(L,t)$, for a representative set of consecutive time-domain symbols as the twin waves propagate through different link distances are shown in Fig. 1c. Similar simulations were carried out for the case of ML-PC.

Transmission performance test. The lasers used in the experiments were external cavity lasers emitting near 1,550 nm with a linewidth of ~100 kHz. The modulators used were PDM I/Q modulators based on $LiNbO_3$ waveguides. For each PDM I/Q modulator, the drive signals were converted to the analogue domain by high-speed DACs operating at up to 64 GSa s^{-1}. Twofold oversampling was used, resulting in a modulation symbol rate of up to 32 Gbaud. The transmission link used for highly dispersive transmission consisted of a recirculating loop, which contained four 80-km fibre spans, each of which could be reconfigured between a SSMF and a TWRS fibre. The average fibre loss at 1,550 nm was 0.21 dB km^{-1}, and the loss of each span was compensated by an EDFA with a noise figure of ~5 dB. The PMD coefficient of the fibres was ~0.1 ps km$^{-1/2}$. A wavelength-selective switch (WSS) was used for gain flattening (within the signal bandwidth). One extra EDFA was used to compensate for the remaining loss in the loop due to the WSS and the optical switch. After fibre transmission, the optical signal was filtered by an optical filter, before being received by a digital coherent receiver. The digital coherent receiver frontend consisted of a 100 kHz linewidth external-cavity laser serving as the OLO, a polarization-diversity 90° optical hybrid for coherent mixing between the received signal and the OLO, four balanced detectors and four 50 GSa s^{-1} analog-to-digital converters (ADCs) in a real-time sampling scope. The four sampled waveforms were stored and processed offline in a computer.

Transmitter and receiver DSP. At the transmitter, the inputs to the DACs were provided by a field-programmable gate array-based real-time logic circuit with stored signal *E*-fields. To generate the signal waveforms, PRBS of length $2^{15}-1$ were first encoded and mapped to signal symbols. Pre-EDC was applied through offline DSP. Additional DSP was applied to partially compensate for the transmitter bandwidth roll-off. At the receiver, the signal processing steps included post-EDC, channel equalization, carrier frequency compensation and carrier phase recovery. The overlap-and-add technique[47] was used for post-EDC. Pilot-assisted single-carrier frequency-domain equalization (PA-SC-FDE)[48,49] was used for channel estimation and compensation, where channel estimation was based on known pilot symbols that are inserted in the payload data sequence in the transmitter. Pilot-assisted multistage phase estimation was used for accurate phase recovery without differential encoding/decoding[49,50]. Note that the additional DSP complexity needed for implementing PCTW is much less than that for a conventional coherent receiver. After signal recovery, decisions were made and BER was obtained by means of error counting. In the case of SD-FEC, the recovered signal waveforms were preprocessed by an SD-FEC decoder before hard decision.

Received 17 October 2012; accepted 5 April 2013;
published online 26 May 2013

References

1. Shannon, C. E. A mathematical theory of communication. *Bell Syst. Tech. J.* **27,** 379–423 (1948).
2. Chraplyvy, A. R. The coming capacity crunch, in *Proceedings of the 2009 European Conference on Optical Communication (Vienna, Austria)*, Plenary Talk (2009).
3. Richardson, D. J. Filling the light pipe. *Science* **330,** 327−328 (2010).
4. Mitra, P. P. & Stark, J. B. Nonlinear limits to the information capacity of optical fibre communications. *Nature* **411,** 1027–1030 (2001).
5. Essiambre, R-J., Foschini, G. J., Kramer, G. & Winzer, P. J. Capacity limits of information transport in fiber-optic networks. *Phys. Rev. Lett.* **101,** 163901 (2008).
6. Shieh, W. & Chen, X. Information spectral efficiency and launch power density limits due to fiber nonlinearity for coherent optical OFDM system. *IEEE Photon. J.* **3,** 158–173 (2011).
7. Liu, X., Wei, X., Slusher, R. E. & McKinstrie, C. J. Improving transmission performance in differential phase-shift-keyed systems by use of lumped nonlinear phase-shift compensation. *Opt. Lett.* **27,** 1616–1618 (2002).
8. Ho, K-P. & Kahn, J. M. Electronic compensation technique to mitigate nonlinear phase noise. *J. Lightwave Technol.* **22,** 779–783 (2004).
9. Roberts, K., Li, C., Strawczynski, L. & O'Sullivan, M. Electronic precompensation of optical nonlinearity. *IEEE Photon. Technol. Lett.* **18,** 403–405 (2006).
10. Johannisson, P., Sjödin, M., Karlsson, M., Tipsuwannakul, E. & Andrekson, P. A. Cancellation of nonlinear phase distortion in self-homodyne coherent systems. *IEEE Photon. Technol. Lett.* **22,** 802–804 (2010).
11. Ip, E. & Kahn, J. M. Compensation of dispersion and nonlinear impairments using digital back propagation. *J. Lightwave Technol.* **26,** 3416–3425 (2008).
12. Mateo, E. F., Zhu, L. & Li, G. Impact of XPM and FWM on the digital implementation of impairment compensation for WDM transmission using backward propagation. *Opt. Express* **16,** 16124–16137 (2008).
13. Yariv, A., Fekete, D. & Pepper, D. M. Compensation for channel dispersion by nonlinear optical phase conjugation. *Opt. Lett.* **4,** 52–54 (1979).
14. Pepper, D. M. & Yariv, A. Compensation for phase distortions in nonlinear media by phase conjugation. *Opt. Lett.* **5,** 59–60 (1980).
15. Fisher, R. A., Suydam, B. R. & Yevick, D. Optical phase conjugation for time-domain undoing of dispersive self-phase-modulation effects. *Opt. Lett.* **8,** 611–613 (1983).
16. Gnauck, A. H., Jopson, R. M. & Derosier, R. M. 10-Gb/s 360-km transmission over dispersive fiber using midsystem spectral inversion. *IEEE Photon. Technol. Lett.* **5,** 663–666 (1993).
17. Watanabe, S., Chikama, T., Ishikawa, G., Terahara, T. & Kuwahara, H. Compensation of pulse shape distortion due to chromatic dispersion and Kerr effect by optical phase conjugation. *IEEE Photon. Technol. Lett.* **5,** 1241–1243 (1993).
18. Chen, X., Liu, X., Chandrasekhar, S., Zhu, B., & Tkach, R. W. Experimental demonstration of fiber nonlinearity mitigation using digital phase conjugation. *Optical Fiber Communication Conference (OFC)*, paper OTh3C.1 (2012).
19. Liu, X. *et al.* Scrambled coherent superposition for enhanced optical fiber communication in the nonlinear transmission regime. *Opt. Express* **20,** 19088–19095 (2012).
20. Agrawal, G. P. *Nonlinear Fiber Optics* (Academic, 2007).
21. Wai, P. K. A., Menyuk, C. R. & Chen, H. H. Stability of solitons in randomly varying birefringent fibers. *Opt. Lett.* **16,** 1231–1233 (1991).
22. Mecozzi, A., Clausen, C. B., Shtaif, M., Park, S-G. & Gnauck, A. H. Cancellation of timing and amplitude jitter in symmetric links using highly dispersed pulses. *IEEE Photon. Technol. Lett.* **13,** 445–447 (2001).
23. Louchet, H., Hodzic, A., Petermann, K., Robinson, A. & Epworth, R. Simple criterion for the characterization of nonlinear impairments in dispersion-managed optical transmission systems. *IEEE Photon. Technol. Lett.* **17,** 2089–2091 (2005).
24. Wei, X. & Liu, X. Analysis of intrachannel four-wave mixing in differential-phase-shift-keyed transmission with large dispersion. *Opt. Lett.* **28,** 2300–2302 (2003).
25. Wei, X. Power-weighted dispersion distribution function for characterizing nonlinear properties of long-haul optical transmission links. *Opt. Lett.* **31,** 2544–2546 (2006).
26. Carena, A., Curri, V., Bosco, G., Poggiolini, P. & Forghieri, F. Modeling of the impact of nonlinear propagation effects in uncompensated optical coherent transmission links. *J. Lightwave Technol.* **30,** 1524–1539 (2012).
27. Vacondio, F. *et al.* On nonlinear distortions of highly dispersive optical coherent systems. *Opt. Express* **20,** 1022–1032 (2012).
28. Slusher R. E. *et al.* Observation of squeezed states generated by four wave mixing in an optical cavity. *Phys. Rev. Lett.* **55**, 2409 (1985).
29. Liu, X., Chandrasekhar, S., Winzer, P. J., Tkach, R. W. & Chraplyvy, A. R. 406.6-Gb/s PDM-BPSK superchannel transmission over 12,800-km TWRS fiber via nonlinear noise squeezing. *Optical Fiber Communication Conference (OFC)*, paper PDP5B.10 (2013).
30. Winzer, P. J. Optical networking beyond WDM. *IEEE Photon. J.* **4,** 647–651 (2012).
31. Liu, X. *et al.* 1.5-Tb/s guard-banded superchannel transmission over 56×100-km (5600-km) ULAF using 30-Gbaud pilot-free OFDM-16QAM signals with 5.75-b/s/Hz net spectral efficiency. *European Conference on Optical Communications (ECOC)*, paper Th3.C.5 (2012).
32. Mizuochi, T. Next generation FEC for optical communication. *Optical Fiber Communication Conference (OFC)*, paper OTuE5 (2008).
33. Schmalen, L. *et al.* A generic tool for assessing the soft-FEC performance in optical transmission experiments. *IEEE Photon. Technol. Lett.* **24,** 40–42 (2012).
34. Chandrasekhar, S., Liu, X., Zhu, B. & Peckham, D. W. Transmission of a 1.2-Tb/s 24-carrier no-guard-interval coherent OFDM superchannel over 7200-km of ultra-large-area fiber. *European Conference on Optical Communications (ECOC)*, paper PD2.6 (2009).

35. Hillerkuss, D. *et al.* 26 Tbit s^{-1} line-rate super-channel transmission utilizing all-optical fast Fourier transform processing. *Nature Photon.* **5,** 364–371 (2011).
36. Tolmachev A. & Nazarathy, M. Filter-bank based efficient transmission of reduced-guard-interval OFDM. *Opt. Express* **19,** B370–B384 (2011).
37. Zhu, B. *et al.* 112-Tb/s space-division multiplexed DWDM transmission with 14-b/s/Hz aggregate spectral efficiency over a 76.8-km seven-core fiber. *Opt. Express* **19,** 16665–16671 (2011).
38. Takara, H. *et al.* 1.01-Pb/s (12 SDM/222 WDM/456 Gb/s) crosstalk-managed transmission with 91.4-b/s/Hz aggregate spectral efficiency. *European Conference on Optical Communications (ECOC)*, paper Th3.C.1 (2012).
39. Wang, J. *et al.* Terabit free-space data transmission employing orbital angular momentum multiplexing. *Nature Photon.* **6,** 488–496 (2012).
40. Foursa D. G. *et al.* Massive terminal dispersion compensation enabling nondispersion-managed submarine links with first generation coherent transponders. *Photon. Technol. Lett.* **24,** 1530–1532 (2012).
41. Tong, Z. *et al.* Towards ultrasensitive optical links enabled by low-noise phase-sensitive amplifiers. *Nature Photon.* **5,** 430–436 (2011).
42. Olsson, S. *et al.* Phase-sensitive amplified optical link operating in the nonlinear transmission regime. *European Conference on Optical Communications (ECOC)*, paper Th.2.F.1 (2012).
43. Lücke, B. *et al.* Twin matter waves for interferometry beyond the classical limit. *Science* **334,** 773–776 (2011).
44. Achilleos, V. *et al.* Multiscale perturbative approach to SU(2)-Higgs classical dynamics: Stability of nonlinear plane waves and bounds of the Higgs field mass. *Phys. Rev. D* **85,** 027702 (2012).
45. Della Negra, M., Jenni, P. & Virdee, T. S. Journey in the search for the Higgs boson: the ATLAS and CMS experiments at the Large Hadron Collider. *Science* **338,** 1560–1568 (2012).
46. CMS Collaboration. A new boson with a mass of 125 GeV observed with the CMS Experiment at the Large Hadron Collider. *Science* **338,** 1569–1575 (2012).
47. Kudo, R. *et al.* Coherent optical single carrier transmission using overlap frequency domain equalization for long-haul optical systems. *J. Lightwave Technol.* **27,** 3721–3728 (2009).
48. Shieh, W., Bao, H. & Tang, Y. Coherent optical OFDM: theory and design. *Opt. Express* **16,** 841–859 (2008).
49. Liu, X. *et al.* M-ary pulse-position modulation and frequency-shift keying with additional polarization/phase modulation for high-sensitivity optical transmission. *Opt. Express* **19,** B868–B881 (2011).
50. Zhou, X. An improved feed-forward carrier recovery algorithm for coherent receiver with M-QAM modulation format. *Photon. Technol. Lett.* **22,** 1051–1053 (2010).

Author contributions

X.L., A.R.C., P.J.W. and R.W.T. jointly developed the concept. X.L. and S.C. designed and performed the experiment. X.L., A.R.C., P.J.W., R.W.T. and S.C. analysed the data. X.L. conducted the theoretical study and wrote the paper.

Additional information

Supplementary information is available in the online version of the paper. Reprints and permissions information is available online at www.nature.com/reprints. Correspondence and requests for materials should be addressed to X.L.

Competing financial interests

The authors have filed two patent applications on the techniques of using phase-conjugated twin waves for improved optical fibre transmission performance: (1) X. Liu, A. R. Chraplyvy, P. J. Winzer & R. W. Tkach, Communication through phase-conjugated optical variants, US patent application no. 13/411462, filed 2 March 2012; (2) X. Liu, A. R. Chraplyvy, P. J. Winzer & R. W. Tkach, Communication through pre-dispersion-compensated phase-conjugated optical variants, US patent application no. 13/601236, filed 31 August 2012.